

Analysis of dielectric optical ring slab waveguides with a layered refractive index

João Torres, António Baptista , *Member, IEEE* , Vitor Maló Machado, *Member, IEEE*

Abstract — A new approach to the analysis of dielectric optical ring slab waveguides with a layered refractive index is developed. Results for a layered approximation of a refractive index with a parabolic profile are presented. Comparison with the well-known results for constant refractive index is performed.

Keywords — ring waveguides, parabolic refractive index, TE propagation modes.

I. INTRODUCTION

Ring waveguides play an important role in photonic integrated circuits. The first propagation models to these waveguides were developed by Marcatili [1] and Marcuse [2]. Since then a lot of work has been done considering waveguides in particular with a constant refractive index profile [1-4].

Recently a generalization of Marcatili's model was presented by the authors [5]. This model is used in this work to treat waveguides with a layered refractive index. In the treated example the layered refractive index tends to a parabolic profile with the increase in the number of layers. The waveguide core is divided into several layers where the refractive index is decreased from the center towards the cladding. Boundary conditions imposed on each layer interface allow the characteristic equation to be obtained. The eigenvalues are numerically calculated from this equation. The profile of TE modes, their confinement in the waveguide core and the curvature losses are calculated for several radii of the ring. The results are analyzed and discussed with regard to published results [4] of structures with a constant refractive index in the core and cladding.

Waveguides with a parabolic profile of the refractive index would be useful in some laser structures, namely separate confinement hetero-structures lasers. The knowledge of their behavior is thus very important for the modelization of these structures. The presented model with an analytical basis is also an important step to the validation of results obtained by numerical methods such as the finite element method for more complex geometries and material properties.

João Torres is a PhD student of Instituto Superior Técnico, Technical University of Lisbon, Portugal (e-mail: joaotorres@ist.utl.pt)

António Baptista is professor at Instituto Superior Técnico, Technical University of Lisbon, Portugal (e-mail: malo.machado@ist.utl.pt)

Vitor Maló Machado is professor at Instituto Superior Técnico, Technical University of Lisbon, Portugal (e-mail: baptista@ist.utl.pt)

II. MODEL

A ring slab waveguide, having cylindrical symmetry, is represented in Fig 1. In our model the material properties do not change in the axial, y , and azimuthal, θ directions. Along the radial direction, however, it is assumed that the refractive index n presents a parabolic variation, simulated by dividing the waveguide into concentric toroidal regions with constant refractive index Fig1b. Due to the waveguide symmetry properties the electromagnetic field does not change in the y direction. Similar to [6], [7] we use Bessel functions to describe the field in the interior medium, a combination of the first and second kind functions in the region inside the cavity and a second kind Hankel function in the region beyond the ring. On the boundaries the field has to be matched imposing the appropriate boundary conditions.

The field is considered to vary harmonically in time satisfying Maxwell equations, in this case with the form:

$$\nabla \times \bar{\mathbf{E}} = -j\omega\mu\bar{\mathbf{H}} \quad (1)$$

$$\nabla \times \bar{\mathbf{H}} = j\omega\varepsilon\bar{\mathbf{E}} \quad (2)$$

$$\nabla \cdot \bar{\mathbf{E}} = 0 \quad (3)$$

$$\nabla \cdot \bar{\mathbf{H}} = 0 \quad (4)$$

where ω , μ and ε are the angular frequency, the magnetic permeability and the dielectric permittivity of the waveguide dielectrics, and $\bar{\mathbf{E}}$, $\bar{\mathbf{H}}$ denote the phasors of the electric and magnetic field strengths, respectively.

In the ring slab waveguide modes the electric and magnetic fields, corresponding to the propagation along the azimuthal direction, are described by [4]:

$$\mathbf{E}(r, \theta, t) = (\tilde{E}_r, \tilde{E}_y, \tilde{E}_\theta)(r)e^{j(\omega t - \gamma R\theta)} \quad (5)$$

$$\mathbf{H}(r, \theta, t) = (\tilde{H}_r, \tilde{H}_y, \tilde{H}_\theta)(r)e^{j(\omega t - \gamma R\theta)} \quad (6)$$

Substituting (5) and (6) into (1)-(4) equations and separating the variables the following results are obtained, as described in [4]:

$$\frac{\gamma R}{r} \tilde{E}_y = -\mu_0 \omega \tilde{H}_r \quad (7)$$

$$\frac{\partial \tilde{E}_y}{\partial r} = -j\mu_0 \omega \tilde{H}_\theta \quad (8)$$

$$\frac{1}{r} \frac{\partial \tilde{E}_\theta}{\partial r} + \frac{j\gamma R}{r} \tilde{E}_r = j\mu_0 \omega \tilde{H}_y \quad (9)$$

and

$$\frac{\gamma R}{r} \tilde{H}_y = \varepsilon_r \varepsilon_0 \omega \tilde{E}_r \quad (10)$$

$$\frac{\partial \tilde{H}_y}{\partial r} = j\epsilon_r \epsilon_0 \omega \tilde{E}_\theta \quad (11)$$

$$\frac{1}{r} \frac{\partial \tilde{H}_\theta}{\partial r} + \frac{j\gamma R}{r} \tilde{H}_r = -j\epsilon_r \epsilon_0 \omega \tilde{E}_y \quad (12)$$

where γ is the propagation constant of the ring slab mode, ϵ_0 the vacuum permittivity and $\epsilon_r = n^2$ the relative permittivity. Due to the energy losses by radiation, the propagation constant is a complex number given by: $\gamma = \beta - j\alpha$, $\beta > 0$, $\alpha > 0$. The real part is the phase coefficient and the imaginary part gives the field damping coefficient. For transverse electric (TE) waves the only nonzero components are \tilde{E}_y , \tilde{H}_r and \tilde{H}_θ which are expressed in terms of \tilde{E}_y . The electromagnetic fields in both TE and TM modes are governed by the following Bessel equation obtained from equations (7) and (8):

$$\frac{\partial^2 \phi}{\partial r^2} + \frac{1}{r} \frac{\partial \phi}{\partial r} + \left(n^2 k^2 - \frac{\gamma^2 R^2}{r^2} \right) \phi = 0 \quad (13)$$

where λ is the vacuum wavelength, n is taken as a constant and $k = 2\pi/\lambda$. Bessel functions, taking $\nu = \gamma R$ as the complex order, are the solution of these equations with $\phi = \tilde{E}_y$ (TE mode). In this work, we are going to analyze only the TE-like modes. The interface conditions for these modes require continuity of E_y and $\partial E_y / \partial r$ across the dielectric interfaces. Since the field must vanish when $r \rightarrow 0$ and $r \rightarrow \infty$, the solution should be a Bessel function of first kind J on the substrate and a Hankel function of second kind on the cladding, where for $r > R$, there is only the contribution of an outward cylindrical wave.

In this way, for a waveguide with a layered refractive index, the solutions of equation (13) for the different regions are given by:

$$\phi(r) = \begin{cases} A_s J_\nu(n_s kr), & \text{if } 0 < r < R-d \\ A_i J_\nu(n_i kr) + B_i Y_\nu(n_i kr), & \text{if } r_{i-1} < r < r_i \\ A_c H_\nu^{(2)}(n_c kr), & \text{if } r > R \end{cases} \quad (14)$$

with A_s , A_i , B_i and A_c determined by the boundary conditions, where i , $i=1, \dots, N$, is the layer order, taking $r_0 = R-d$ and $r_N = R$.

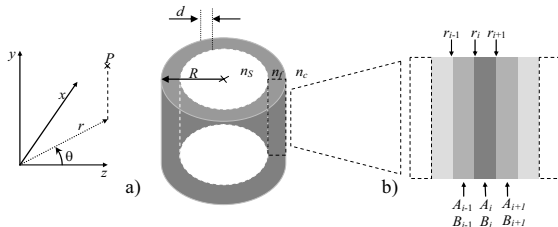


Fig 1. a) A ring slab waveguide. b) Cavity partition into several layers with equal width. A_i , B_i are the field coefficients in the layer of order i .

The ring slab cavity with thickness d is embedded between an interior medium (s) with refractive index n_s and an exterior medium (c) with refractive index $n_c = n_s$ (Fig.1a). The distance between the origin and the outer rim of the ring defines the ring radius R .

A standard parabolic profile with the inflection point at the center of the cavity ($r = R-d/2$) with index n_f , and a refractive index n_s at the positions $r < R$ and $r > R-d$, was used to describe the refractive index variation with r , $n(r)$. The ring slab (Fig.1b) was divided into several layers ($i=1, \dots, N$) of equal thickness. The problem is treated considering a step approximation of the refractive index profile. For this aim, the index of each layer i was taken as the value of $n(r)$ at the center position of the layer $(r_{i-1} + r_i)/2$.

Boundary conditions in each interface lead to a homogeneous system of $2(N+1)$ linear equations for the coefficients $A_s, A_1, B_1, \dots, A_N, B_N, A_c$ to which it is necessary to add the propagation constant ν . Thus, all the constants $A_s, A_c, A_i, B_i, i=1, \dots, N$, will be determined except one (A_s) which may be arbitrarily imposed.

The time average power flow density is given by the real part of the complex Poynting vector $\mathbf{S}_{av} = \frac{1}{2} \Re[\mathbf{E} \times \mathbf{H}^*]$. The components of this quantity for the TE-mode along the r and θ coordinates are respectively given by:

$$S_{av,r} = -\frac{1}{2\mu_0\omega} \Re \left[j \tilde{E}_y \frac{\partial \tilde{E}_y}{\partial r} \right] e^{-2\alpha R\theta} \quad (15)$$

$$S_{av,\theta} = \frac{\beta}{2\mu_0\omega} \frac{R}{r} |\tilde{E}_y|^2 e^{-2\alpha R\theta} \quad (16)$$

Then, it is possible to determine the total optical average value of the power per unit length, carried by the wave travelling in the azimuthal direction:

$$P_\theta(\theta) = \int_0^\infty S_{av,\theta} dr = \frac{\beta R}{2\mu_0\omega} e^{-2\alpha R\theta} \int_0^\infty \frac{|E_y|^2}{r} dr \quad (17)$$

It is possible to achieve all the constants A_c, A_i, B_i as a function of the constant A_s . This means that:

$$P_\theta(\theta) \propto |A_s|^2 \Rightarrow \sqrt{P_\theta(\theta)} \propto |A_s| \quad (18)$$

Result of equation (18) will be used to define energetically the normalized factor for the electric field strength which is taken as $\sqrt{\mu_0\omega P_\theta(\theta)}$. The ratio \mathcal{G} between the power flow in the azimuthal direction inside the ring and the power flow in all range is used as a measurement of the mode confinement:

$$\mathcal{G} = \frac{\int_{R-d}^R S_{av,\theta} dr}{P_\theta(\theta)} \quad (19)$$

The curvature losses correspond to the power flow in the radial direction:

$$P_r(r) = \int_0^{2\pi} S_{av,r} r d\theta \quad (20)$$

III. RESULTS

A numerical technique similar to the one described in [4] was used to find the roots of the characteristic equation in the complex plane. The discrete approximation of the refractive index tends to the parabolic profile when the number of layers increases. A good approximation is obtained when the number of layers is equal or greater than eleven. The refractive index outside the ring slab is 1.6 and the maximum index inside the ring slab is 1.7. The wavelength used is $\lambda=1.3\mu\text{m}$.

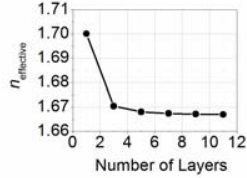


Fig.2. Effective refractive index as a function of the number of layers inside the cavity.

The validation of our results concerning the angular propagation constant ν was done by comparison with those of [4], [8] for the eigenvalue associated with the fundamental mode with one layer and $d=1\mu\text{m}$. As a consequence of the equivalence of the algorithms, we found an excellent agreement showing a deviation less than 1% compared to the results presented in [4] and [8].

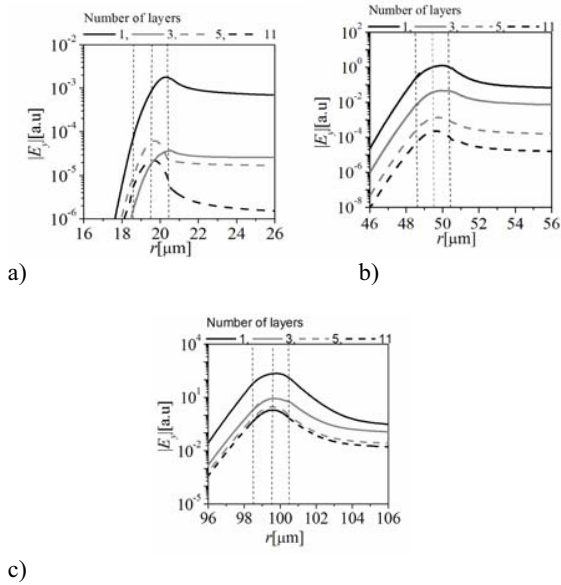


Fig.3. TE_0 mode profiles for three different radius: a) $R=20.5\mu\text{m}$ b) $R=50.5\mu\text{m}$ and c) $R=100.5\mu\text{m}$ for several layers used inside the cavity.

With the reduction of R , Fig.3, the maximum absolute value of the basic electric field shifts towards the outer rim of the ring slab, and the relative field levels in the exterior region grow. However when the number of layers grows the maximum tends to the center of the ring slab, showing the importance of the mode confinement for small radius, and the absolute value of the field decreases, as a consequence of the effective refractive index decrease

(Fig.2). It is also observed, as expected, that ring waveguides with large radii R support modes with the familiar symmetric profile, which is characteristic of straight symmetric slab waveguides [8].

In Fig.4 it is interesting to look at the behavior of the complex amplitude of the field with the full range of the radial coordinate. When $r=0$ the complex amplitude is null. Inside the cavity the complex amplitude is almost real, reaching a maximum in its interior. Outside the cavity, the field has real and imaginary parts with damping oscillations in the radial direction. Analyzing the plots of Fig.3 it is also possible to see a decrease in the amplitude of the oscillations, with the number of layers, for both values of R . Also there is a decrease in amplitude of the oscillations with the distance to the ring slab. However for $R=20.5\mu\text{m}$ and eleven layers there is a small variation as can be seen in Fig.3a) and Fig.4a).

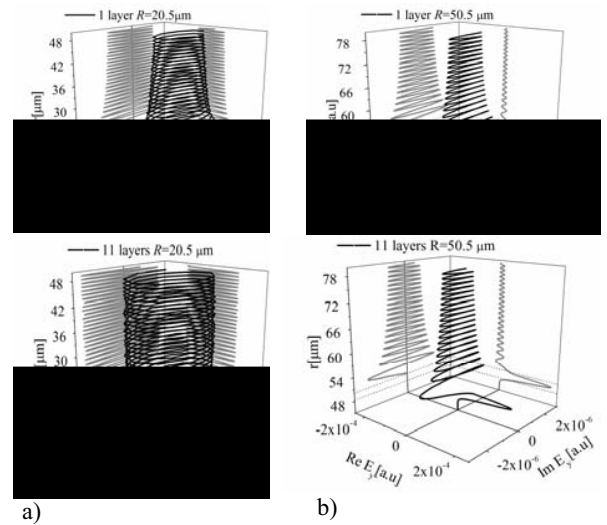


Fig.4. Complex amplitude of the field for two radius of curvature (black lines). Gray lines, represent projections on the planes. Dashed lines depict inside and outside limits of the cavity. In Fig a) the plots show the field behavior for a radius of $20.5\mu\text{m}$ and in Fig b) for a radius of $50.5\mu\text{m}$.

To understand this behavior let's take a look at the parameter characterizing the confinement of the field mode.

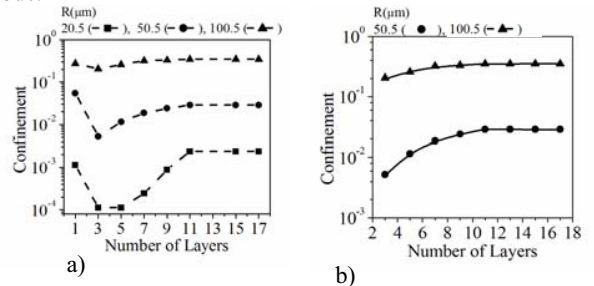


Fig.5. (a) Confinement for the three situations $R=100.5$, 50.5 , $20.5\mu\text{m}$. (b) Confinement fitting to the curves with $R=100.5$, $50.5\mu\text{m}$.

In Fig.5a it is shown that there is a minimum value of

the confinement for 3 layers.

This result can be explained based on the two mechanisms that affect the parameter in opposite directions. The first one is the reduction in the effective refractive index, see Fig.2. The other one is a consequence of the maximum value location of the field which is a consequence of the refractive index profile. The importance of this effect grows with the number of layers. The first one tends to reduce the energy confined in the ring; the second one tends to increase that energy. When the number of layers grows from one to three the effective refractive index has a sudden and important decrease. The result is a reduction in the confinement mode parameter. Raising the number of layers the decrease of the effective refractive index becomes unimportant and the energy confined in the ring grows even more with the number of layers. This behavior can be confirmed looking at the shift of the field maximum value. When the number of layers passes from one to three there is almost no change in the maximum position but for a number of layers greater than three this maximum value deviates to the center of the waveguide ring. Results for the curves with $R=100.5$, $50.5\mu\text{m}$ (Fig.5b) were fitted with an exponential function

The variation of the power radiated through the outer ring surface with the number of layers inside the ring slab and the radius is also presented in, Fig.6. As expected, the power radiated is sensitive to the radius. With small radius the radiated power is greater than with greater ones. The radiated power is directly related to the curvature losses. When the confinement is increased the curvature losses are decreased. On the other hand, the same quantity, the power radiated along the radial direction, calculated through the inner ring surface gives a result which can be neglected showing that the curvature losses correspond essentially to the radiated field towards outside the ring.

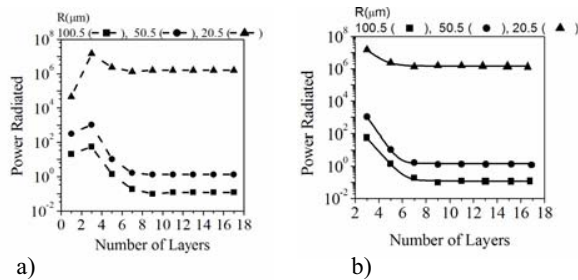


Fig.6. (a) Power radiated at a distance of $R_0=1000 \mu\text{m}$ of the cavity as a function of the number of layers. $R=100.5$, 50.5 , $20.5\mu\text{m}$; (b) curve fitting of the power radiated when the number of layers is greater than three.

Power radiated was also fitted (Fig.6.b) with an exponential function.

IV. CONCLUSION

An analytical approach to the analysis of two-dimensional ring slab waveguides has been presented. The ring waveguide mode profiles, confinement and curvature losses were calculated when the refractive index presents a parabolic variation. The model approximates the refractive index function by a set of layers. The calculation of the

field results from the model equations through the imposition of boundary conditions in each layer interface, followed by the determination of the overall system eigenvalues.

The following conclusions may be extracted:

1. The TE₀ mode profile has an interesting evolution in the guide. Without steps, the mode profile of a ring waveguide is asymmetric and their maximum value is near the outer frontier of the guide. When the number of layers, increases the maximum value of the mode profile tends to the center of the waveguide and the profile tends to a symmetric one, as it appears in a straight waveguide. This behavior is related to the diminishing of the curvature losses.
2. The confinement passes through a minimum value, Fig.5. This value is determined by two opposite factors acting on the confinement: one is the diminishing of the effective refractive index and the other one the increasing of the number of layers N and the consequent diminishing of the curvature losses, corresponding to the confinement increasing. When $R>50\mu\text{m}$ and $N>3$ it was showed how the confinement function can be approximated using a exponential function.
3. The power radiated has a maximum value when the confinement passes through a minimum (corresponding to a maximum value for the curvature losses), which can also be described by an exponential function.

ACKNOWLEDGMENT

The author acknowledges the FCT by the financial support of the project PTDC/EEA -ELC/69515/2006

REFERENCES

- [1] E. A. J. Marcanti, "Bends in optical dielectric guides," *Bell Syst. Tech. J.*, vol. 48, pp. 2103-2132, Sept. 1969.
- [2] D. Marcuse, "Bending losses of the asymmetric slab waveguide", *Bell Syst. Tech. J.*, vol. 50, pp. 2551-2563, Oct. 1971.
- [3] M. Heiblum and J. H. Harris, "Analysis of curved optical waveguides by conformal transformation", *IEEE J. Quantum Electron.*, vol. QE-11, pp. 75-83, Feb. 1975.
- [4] K. R. Hiremath, M. Hammer, R. Stoffer, L. Prkna and J. Ctyroky, "Analytic approach to dielectric optical bent slab waveguides", *Optical and Quantum Electronics*, vol. 37(1-3), pp. 37-61, Jan 2005.
- [5] J. Torres, António Baptista, Vitor Maló Machado, "Curvature losses of slab waveguides using analytical and FEM analysis", presented at ODF 2010, 7th International Conference on Optics-photonics Design & Fabrication, Yokohama, Japan, April 19-21, 2010, paper 20PSa-40.
- [6] B. M. Azizur Rahman, J Brian Davies, "Finite-Element Analysis of Optical and Microwave Waveguide Problems", *IEEE Trans. Microwave Theory Tech.* vol. MTT-32, pp. 20-28, Jan 1984.
- [7] D. Marcuse. *Light Transmission Optics*. Van Nostrand Reinhold Company, New York, 1972.
- [8] C. Vassallo. *Optical Waveguide Concepts*. Elsevier, Amsterdam, 1991.